Journal of Thermal Analysis and Calorimetry, Vol. 58 (1999) 103-111

THERMAL STABILITY OF SOME POLYNUCLEAR COORDINATION COMPOUNDS IN THE SYSTEMS Ln(III)–Co(II)–OXALATE

M. Badea[1], *R. Olar*[1], *E. Cristurean*[1], *D. Marinescu*[1],
M. Brezeanu[1], *M. Balasoiu*[2] *and E. Segal*[3]

[1]Department of Inorganic Chemistry, Bucharest University, 23 Dumbrava Rosie St.
Bucharest
[2]Institute of Physical Chemistry, 202, Spl. Independentei, RO-77208, Bucharest
[3]Department of Physical Chemistry, University of Bucharest, Bulevardul Elisabeth 4-12
Bucharest, Romania

(Received January 10, 1998; in revised form September 5, 1998)

Abstract

This paper reports an investigation of the thermal stabilities of the class of coordination compounds containing lanthanide ions Ln(III) (*Ln*=La, Sm, Eu, Dy, Er), Co(II) ions and oxalate anions $C_2O_4^{2-}$. The thermal decomposition steps were identified, and in some cases the values of the non-isothermal kinetic parameters were determined.

Keywords: Ln(III)–Co(II) coordination compounds, non-isothermal kinetics, thermal stability

Introduction

The controlled thermal decomposition of polynuclear coordination compounds is used to obtain mixed oxides with spinel and perowskite structures.

Following research on the thermal stability and non-isothermal decomposition kinetics of coordination compounds [1–7], this paper presents results on five polynuclear coordination compounds involving mixed oxalates of lanthanides and cobalt(II).

Experimental

The coordination compounds (**I**)–(**V**) were synthesized and characterized via elemental chemical analysis, electronic and vibration spectra and magnetic susceptibility measurements [8].

The thermal decomposition curves were recorded with a Paulik-Paulik-Erdey derivatograph (MOM, Budapest) in the temperature range 20–1000°C at heating rates in the range 2.7–10 K min^{-1}.

X-ray diffractograms were recorded with a Phillips P. W. 1140 X-ray diffractometer, using CrK_α radiation.

1418–2874/99/ $ 5.00

Akadémiai Kiadó, Budapest
Kluwer Academic Publishers, Dordrecht

In order to estimate the mean sizes of crystallites, Scherrer's formula [9] was applied. For evaluation of the non-isothermal kinetic parameters, the integral methods of Coats-Redfern [10], Flynn-Wall (for constant heating rate) [11] and Coats-Redfern as modified by Urbanovici-Segal [12] were used.

The experimental data were processed with the program Versatile written in Basic language by Dragoe and Segal [13]. The program yields the values of the kinetic parameters, and allows simulation of the TG curves in the coordinates (α, T/C^o), α being the degree of conversion, and their fitting to the experimental points. In this way, the correctness of the determined values of the non-isothermal kinetic parameters is checked.

Results and discussion

The following solid coordination compounds were prepared and studied:

$LaCo(C_2O_4)_{2.5}\cdot 6H_2O$ (**I**)
$SmCo(C_2O_4)_{2.5}\cdot 4H_2O$ (**II**)
$EuCo(C_2O_4)_{2.5}\cdot 9H_2O$ (**III**)
$DyCo(C_2O_4)_{2.5}\cdot 10H_2O$ (**IV**)
$ErCo(C_2O_4)_{2.5}\cdot 6H_2O$ (**V**)

The general molecular formula of these compounds is

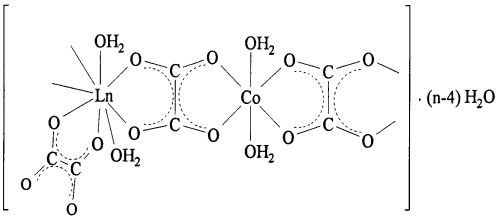

Ln=La, n=6; Ln=Sm, n=4; Ln=Eu, n=9; Ln=Dy, n=10; Ln=Er; n=6

Table 1 presents results obtained from an analysis of the X-ray powder diffraction data on the investigated compounds.

Thermal decomposition of $LaCo(C_2O_4)_{2.5}\cdot 6H_2O$

The TG curve indicated the following decomposition steps:

$$LaCo(C_2O_4)_{2.5}\cdot 6H_2O_{(s)} \xrightarrow{115^oC} LaCo(C_2O_4)_{2.5}\cdot 2H_2O_{(s)} + 4H_2O_{(g)} \qquad (1)$$

$$LaCo(C_2O_4)_{2.5}\cdot 2H_2O_{(s)} \xrightarrow{165^oC} LaCo(C_2O_4)_{2.5(s)} + 2H_2O_{(g)} \qquad (2)$$

As shown by the DTA curve, reactions (1) and (2) are accompanied by endothermic effects.

Table 1 Relative intensities, interplanar distances and mean crystallite sizes of the investigated compounds

Compound	*d*/Ĺ	Relative intensity	*l*/Ĺ
$LaCo(C_2O_4)_{2.5}\cdot 6H_2O$ (**I**)	5.69	45	
	5.39	64	
	4.84	36	
	4.55	92	
	4.43	92	
	4.23	85	
	3.94	100	30.86
	3.57	64	
	3.38	63	
	2.83	81	
	2.63		
$SmCo(C_2O_4)_{2.5}\cdot 4H_2O$ (**II**)	4.80	63	
	4.62	100	30.47
	4.45	36	
	4.28	32	
	4.15	43	
	3.97	25	
	3.34	51	
	3.32	67	
	3.14	34	
	2.80	37	
	2.76	51	
	2.72	69	
	2.38	43	
$EuCo(C_2O_4)_{2.5}\cdot 9H_2O$ (**III**)	5.62	28	
	5.22	95	
	5.06	55	
	4.83	46	
	4.66	56	
	4.45	69	
	4.21	92	

Table 1 Continued

Compound	*d*/Ĺ	Relative intensity	*l*/Ĺ
$EuCo(C_2O_4)_{2.5}\cdot 9H_2O$ (**III**)	3.93	97	63.48
	3.34	79	
	3.30	92	
	3.12	100	
	3.01	87	
	2.79	93	
	2.64	70	
	2.60	67	
$DyCo(C_2O_4)_{2.5}\cdot 10H_2O$ (**IV**)	5.62	71	30.55
	5.24	59	
	4.78	70	
	4.68	72	
	4.46	100	
	4.23	57	
	3.98	83	
	3.57	75	
	3.31	45	
	2.79	63	
	2.64	46	
	2.59	41	
$ErCo(C_2O_4)_{2.5}\cdot 6H_2O$ (**V**)	5.64	67	30.67
	5.29	78	
	4.45	92	
	4.23	100	
	3.96	64	
	3.58	54	
	3.35	72	
	2.85	40	
	2.63	65	

In the strongly exothermic third step, a mixed carbonate is generated:

$$2\mathrm{LaCo(C_2O_4)_{2.5(s)}} \xrightarrow{245^\circ\mathrm{C}} 2\mathrm{LaCo(CO_3)_{2.5(s)}} + 5\mathrm{CO_{(g)}} \tag{3}$$

During the fourth step an oxocarbonate is formed:

$$2\mathrm{LaCo(CO_3)_{2.5(s)}} \xrightarrow{370^\circ\mathrm{C}} 2\mathrm{LaCo(CO_3)O_{1.5(s)}} + 3\mathrm{CO_{2(g)}} \tag{4}$$

In the last decomposition step, which is also strongly exothermic, the mixed oxide with perowskite structure is obtained:

$$2\mathrm{LaCo(CO_3)O_{1.5(s)}} + 1/2\mathrm{O_{2(g)}} \xrightarrow{630^\circ\mathrm{C}} 2\mathrm{LaCoO_{3(s)}} + 2\mathrm{CO_{2(g)}} \tag{5}$$

This compound is stable up to 900°C.

At higher temperatures, it decomposes into La_2O_3 and Co_3O_4, as shown by the X-ray diffractograms (Figs 1 and 2).

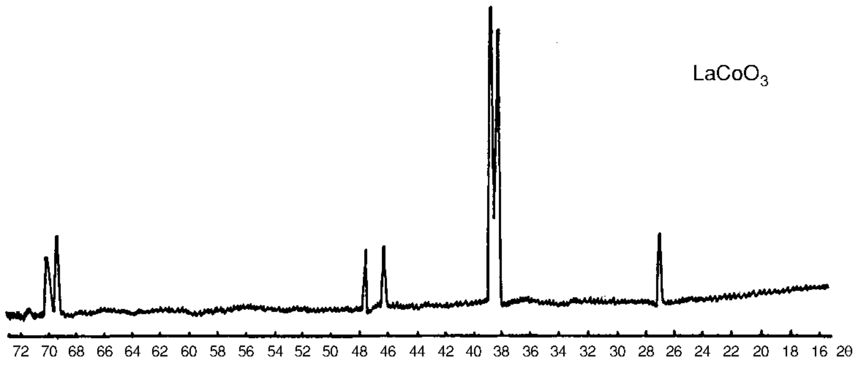

Fig. 1 Diffractogram of $LaCoO_3$

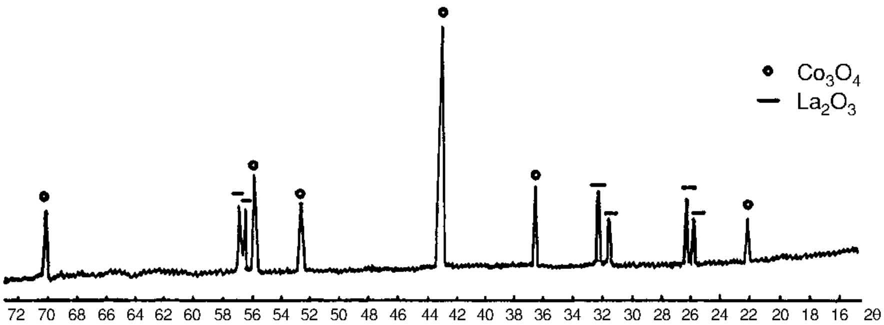

Fig. 2 Diffractogram of mixture of La_2O_3 and Co_3O_4

In Eqs (1)–(5), the temperatures written above the arrows correspond to the maximum rates (peaks of the DTG curves) at a heating rate, β, of 2.78 K min^{-1}.

Table 2 Values of the non-isothermal kinetic parameters of reaction (1) at β=2.78 K min^{-1}

Methods	n	E/kJ mol^{-1}	A/s^{-1}	$\lvert r \rvert$*
Coats-Redfern	1.4	117.6	$4.04\cdot10^{13}$	0.999
Flynn-Wall	1.4	117.7	$4.15\cdot10^{13}$	0.999
Modified Coats-Redfern	1.2	116.3	$2.64\cdot10^{13}$	0.999

* Correlation coefficient of linear regression

For reaction (1), the values of the non-isothermal kinetic parameters are listed in Table 2.

Thermal decomposition of $SmCo(C_2O_4)_{2.5}\cdot4H_2O$

Decomposition to the mixed oxide proceeds in the following steps:

$$SmCo(C_2O_4)_{2.5}\cdot4H_2O_{(s)} \xrightarrow{135^{\circ}C} SmCo(C_2O_4)_{2.5}\cdot2H_2O_{(s)} + 2H_2O_{(g)} \tag{6}$$

$$SmCo(C_2O_4)_{2.5}\cdot2H_2O_{(s)} \xrightarrow{178^{\circ}C} SmCo(C_2O_4)_{2.5(s)} + 2H_2O_{(g)} \tag{7}$$

$$2SmCo(C_2O_4)_{2.5(s)} \xrightarrow{260^{\circ}C} 2SmCo(CO_3)_{2.5(s)} + 5CO_{(g)} \tag{8}$$

$$2SmCo(CO_3)_{2.5(s)} \xrightarrow{390^{\circ}C} 2SmCo(CO_3)_2O_{0.5(s)} + CO_{2(g)} \tag{9}$$

$$2SmCo(CO_3)_2O_{0.5(s)} \xrightarrow{430^{\circ}C} 2SmCo(CO_3)_{0.5}O_{2(s)} + 3CO_{2(g)} \tag{10}$$

$$2SmCo(CO_3)_{0.5}O_{2(s)} + 1/2O_{2(g)} \xrightarrow{465\text{–}630^{\circ}C} 2SmCoO_{3(s)} + CO_{2(g)} \tag{11}$$

The first three decomposition steps are endothermic; the others are exothermic.

The solid residue obtained at 630°C consists of the mixed oxide with perowskite structure. At temperatures higher than 900°C, this compound decomposes to the simple oxides.

Thermal decomposition of $EuCo(C_2O_4)_{2.5}\cdot9H_2O$

This compound exhibits the following decomposition steps:

$$EuCo(C_2O_4)_{2.5}\cdot9H_2O_{(s)} \xrightarrow{90^{\circ}C} EuCo(C_2O_4)_{2.5}\cdot6H_2O_{(s)} + 3H_2O_{(g)} \tag{12}$$

$$EuCo(C_2O_4)_{2.5}\cdot6H_2O_{(s)} \xrightarrow{170^{\circ}C} EuCo(C_2O_4)_{2.5}\cdot2H_2O_{(s)} + 4H_2O_{(g)} \tag{13}$$

$$EuCo(C_2O_4)_{2.5}\cdot2H_2O_{(s)} \xrightarrow{202^{\circ}C} EuCo(C_2O_4)_{2.5}(s) + 2H_2O_{(g)} \tag{14}$$

$$2EuCo(C_2O_4)_{2.5(s)} \xrightarrow{265^{\circ}C} 2EuCo(CO_3)_{2.5}(s) + 5CO_{(g)} \tag{15}$$

→

$$2\mathrm{EuCo(CO_3)_{2.5(s)}} + 1/2\mathrm{O_{2(g)}} \xrightarrow{300\text{–}625^\circ\mathrm{C}} 2\mathrm{EuCoO_{3(s)}} + 5\mathrm{CO_{2(g)}} \qquad (16)$$

The solid residue obtained at 625°C, which is the mixed oxide with perowskite structure, undergoes further decomposition to the simple oxides at temperatures higher than 900°C.

The values of the non-isothermal kinetic parameters for the reaction described by Eq. (12) are listed in Table 3.

Table 3 Values of the non-isothermal kinetic parameters of reaction (12) at β=2.78 K min^{-1}

Method	n	E/kJ mol^{-1}	A/s^{-1}	$\|r\|$*
Coats-Redfern	1.5	135.8	$8.09\cdot10^{15}$	0.999
Flynn-Wall	1.5	134.9	$6.07\cdot10^{16}$	0.999
Modified Coats-Redfern	1.4	141.9	$6.88\cdot10^{17}$	0.997

* Correlation coefficient of linear regression

As in the former case, reasonably satisfactory agreement was observed between the values obtained with the three integral methods.

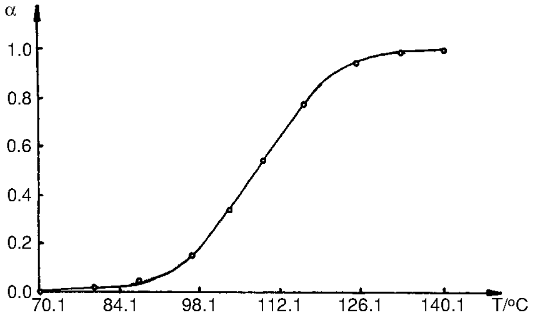

Fig. 3 Simulated thermogravimetric curve, using coordinates α, T (°C) for reaction (1); —– calculated curve, ○ – experimental points

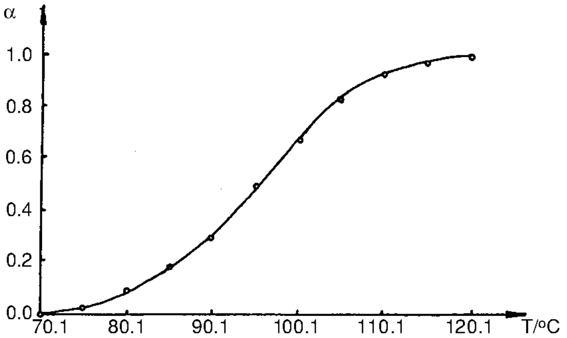

Fig. 4 Simulated thermogravimetric curve, using coordinates α, T (°C) for reaction (12); —– calculated curve, ○ – experimental points

Figures 3 and 4 show the simulated (α, T, °C) curves obtained with the Coats-Redfern values of the non-isothermal kinetic parameters, and the experimental points, which practically lie on the curves. This is further proof of the correctness of the obtained values of the non-isothermal kinetic parameters.

Thermal decomposition of $DyCo(C_2O_4)_{2.5}\cdot 10H_2O$

The following thermal decomposition steps were indicated:

$$\mathrm{DyCo(C_2O_4)_{2.5}\cdot 10H_2O_{(s)}} \xrightarrow{60^{\circ}\mathrm{C}} \mathrm{DuCo(C_2O_4)_{2.5}\cdot 7H_2O_{(s)} + 3H_2O_{(g)}} \qquad (15)$$

$$\mathrm{DyCo(C_2O_4)_{2.5}\cdot 7H_2O_{(s)}} \xrightarrow{138^{\circ}\mathrm{C}} \mathrm{DyCo(C_2O_4)_{2.5}\cdot 4H_2O_{(s)} + 3H_2O_{(g)}} \qquad (16)$$

$$\mathrm{DyCo(C_2O_4)_{2.5}\cdot 4H_2O_{(s)}} \xrightarrow{175^{\circ}\mathrm{C}} \mathrm{DyCo(C_2O_4)_{2.5}\cdot 2H_2O_{(s)} + 2H_2O_{(g)}} \qquad (17)$$

$$\mathrm{DyCo(C_2O_4)_{2.5}\cdot 2H_2O(s)} \xrightarrow{221^{\circ}\mathrm{C}} \mathrm{DyCo(C_2O_4)_{2.5\,(s)} + 2H_2O_{(g)}} \qquad (18)$$

$$\mathrm{2DyCo(C_2O_4)_{2.5\,(s)}} \xrightarrow{270^{\circ}\mathrm{C}} \mathrm{2DyCo(CO_3)_{2.5(s)}) + 5CO_{(g)}} \qquad (19)$$

$$\mathrm{2DyCo(CO_3)_{2.5(s)} + 1/2O_{2\,(g)}} \xrightarrow{422\text{–}520^{\circ}\mathrm{C}} \mathrm{2DyCoO_{3(s)} + 5CO_{2\,(g)}} \qquad (20)$$

The solid residue with perowskite structure is obtained at 520°C. It decomposes into the simple oxides at temperatures higher than 900°C.

Thermal decomposition of $ErCo(C_2O_4)_{2.5}\cdot 6H_2O$

In this case, the following four thermal decomposition steps were observed:

$$\mathrm{ErCo(C_2O_4)_{2.5}\cdot 6H_2O_{(s)}} \xrightarrow{55\text{–}95^{\circ}\mathrm{C}} \mathrm{ErCo(C_2O_4)_{2.5}\cdot 4H_2O_{(s)} + 2H_2O_{(g)}} \qquad (21)$$

$$\mathrm{ErCo(C_2O_4)_{2.5}\cdot 4H_2O_{(s)}} \xrightarrow{170^{\circ}\mathrm{C}} \mathrm{ErCo(C_2O_4)_{2.5(s)}) + 4H_2O_{(g)}} \qquad (22)$$

$$\mathrm{2ErCo(C_2O_4)_{2.5(s)}} \xrightarrow{275^{\circ}\mathrm{C}} \mathrm{2ErCo(CO_3)_{2.5(s)} + 5CO_{(g)}} \qquad (23)$$

$$\mathrm{ErCo(CO_3)_{2.5(s)} + 1/2O_{2(g)}} \xrightarrow{395\text{–}500^{\circ}\mathrm{C}} \mathrm{2ErCoO_{3(s)} + 5CO_{2(g)}} \qquad (24)$$

In this case too, the mixed oxide is obtained at a relatively low temperature (500°C). At temperatures higher than 900°C, this compound undergoes decomposition to the simple oxide.

For all the investigated compounds, the thermal degradation of the oxalate ligand occurs in a narrow temperature range (maximum 10°C). The corresponding temperatures increase in the following sequence:

La(III) (245°C) < Sm(III) (260°C) < Eu(III) (265°C) < Dy(III) (270°C)
< Er(III) (275°C)

This is experimental evidence of the increase in thermal stability and ligand – metal ion bond strength with decrease in the ionic radius. The interaction of Ln(III) (a strong acid – class a) with the ligand $C_2O_4^{2-}$ (a strong base – class a) exhibits a strong electrostatic character; thus, the metal – ligand bond energy increases with decrease in the ionic radius.

Conclusions

The thermal decomposition steps of five polynuclear coordination compounds were established, and for two steps the non-isothermal kinetic parameters were determined by three integral methods. The correlation between the thermal stability and the metal – ligand bond energy is inferred.

References

1 M. Brezeanu, L. Patron, E. Cristurean, D. Marinescu, A. Antoniu, M. Andruh, O. Carp, N. Stanica and A. Gheorghe, Rev. Roum. Chim., 38 (1993) 1173.
2 M. Brezeanu, L. Patron, E. Cristurean and O. Carp, Rev. Roum. Chim., (in press).
3 M. Brezeanu, E. Cristurean, D. Pogorevici, E. Segal, D. Marinescu, O. Carp, M. Andruh and S. Ciobanu, Anal. Univ. Buc., 1 (1992) 15.
4 M. Brezeanu, E. Cristurean, E. Pincovschi and N. Popa, Anal. Univ. Buc., 2 (1993) 9.
5 M. Brezeanu, A. Antoniu, E. Cristurean, C. Draghici, M. Andruh and M. Badea, Anal. Univ. Buc., 2 (1993) 13.
6 M. Brezeanu, D. Marinescu, M. Badea, C. Ciomaga, N. Stanica and D. Stefanescu, Rev. Roum. Chim., (in press).
7 M. Brezeanu, E. Cristurean and L. Patron, Rev. Roum. Chim., (in press).
8 M. Brezeanu, M. Badea, E. Cristurean, D. Marinescu and R. Olar, Rev. Roum. Chim., (in press).
9 A. Guinier, Théorie et Technique de la Radiocristallographie, Dunod, Paris 1964, p. 462.
10 A. W. Coats and J. P. Redfern, Nature, 201 (1964) 68.
11 F. H. Flynn and L. A. Wall, Polym. Lett., 4 (1966) 323.
12 E. Urbanovici and E. Segal, Thermochim. Acta, 81 (1984) 379.
13 N. Dragoe and E. Segal, Thermochim. Acta, 185 (1991) 129.